Quinolinium-Derived Acentric Crystals for Second-Order NLO Applications with Transparency in the Blue

Alexander Zelichenok, Vladimir Burtman, Noemi Zenou, and Shlomo Yitzchaik*

Department of Inorganic and Analytical Chemistry, The Hebrew University of Jerusalem, Jerusalem 91904, Israel

Santo Di Bella*

Department of Chemistry, University of Catania, Catania 95125, Italy

Guilia Meshulam and Zvi Kotler

NLO Group, Soreq Nuclear Research Center, Yavne 81800, Israel

Received: May 19, 1999; In Final Form: August 4, 1999

Derivatives of quinolinium iodide have been found to exhibit second-order nonlinear optical (NLO) response in their crystalline form. The quaternary amine functionality is introduced as an electron-withdrawing group in NLO-active chromophores. While their electron-accepting capabilities are somewhat weaker than those of the nitro group, these organic salts show a much more favorable transparency−nonlinearity tradeoff for blue second harmonic generation (SHG) NLO applications. Here we present crystal growth and characterization via X-ray diffraction (XRD), NMR, FTIR, and optical spectroscopy measurements. Experimental linear optical features are fully consistent with INDO/SCI−SOS theoretical calculations. These latter provide a rationale for the NLO response of these materials. Calculations predict a sizable molecular nonlinearity, which parallels the wavelength of the lowest charge-transfer transition. In addition, a direct correlation between SHG powder response to the β crystallographic angle is observed.

Introduction

Single crystals containing hyperpolarizable chromophores which are packed in a noncentrosymmetric space group are among the most promising bulk materials for nonlinear optical applications.[1] They are widely studied because of their large nonlinear optical (NLO) coefficients and their maximized chromophore number densities and orientation temporal stability, as compared with poled polymers.[2] The NLO response arises from the hyperpolarizable constituent chromophores, which are macroscopically aligned in a polar manner, and thus the response of the individual molecules adds constructively.

Within the past few years, organic materials for nonlinear optics attracted increasing attention due to the remarkable growth of photonics technologies such as optical data storage, fast optical switches, and others.[3] New organic materials susceptible for use in diode lasers frequency doubling are especially requested. Although inorganic crystals, such as $LiNbO_3$ or KH_2PO_4, have proven their efficiency in frequency conversion, high expenditures, thin film processability, and hygroscopic properties of these materials prevented a wider use. In contrast, organic materials exhibit larger nonlinear optical coefficients and also have the advantage of higher synthetic flexibility. Organic synthesis allows a new level of molecular design to be employed in which molecular assemblies are controlled by characteristics of individual substituent groups, to optimize the nonlinear optical properties. Realization of bulk materials having large macroscopic second-order nonlinear optical response, $\chi^{(2)}$, requires not only molecular constituents with large microscopic second-order molecular susceptibility, β_{ijk}, but also macroscopic noncentrosymmetric packing of the assemblies, aligned in a manner that the individual tensor components of β_{ijk} add constructively.[4,5] However, one of the serious problems connected with frequency doubling for organic materials is their transparency at the second harmonic wavelength at about 415 nm for the fundamental wavelength, 830 nm, diode laser. This problem may be overcome by creation of material with cutoff transparency at about 400 nm.[6]

SCHEME 1

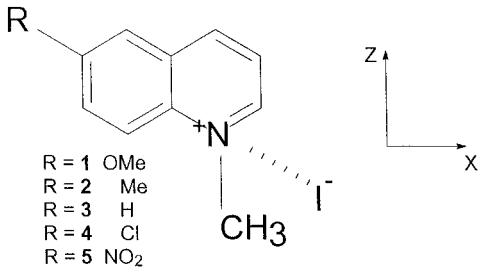

In this contribution, we report a new class of organic NLO materials based on a systematic study of donor−acceptor substituted quinolinium salts, as illustrated in Scheme 1. We demonstrate the ability of the quaternary ammonium salt to serve as a strong acceptor with electron-withdrawing capabilities similar to that of nitro group with a remarkable blue-shifted absorption leaving a transparency window in the blue. The isoquinolines have already been studied as nonlinear optical chromophores.[7]

10.1021/jp991616h CCC: $18.00
Published on Web 09/29/1999

Experimental Section

The syntheses of all investigated materials were carried out as described previously.[8] Except the case of 6-dimethylamino quinoline, which we did not succeed in obtaining in a considerable amount due to some practical limitations of the Skraup synthesis.[9]

Crystal growth was carried out by slow evaporation of water-saturated solutions of the appropriate compound. ^{1}H NMR spectra were measured on a AMX 400 Bruker spectrometer in D_2O or DMSO-d_6 using tetramethylsilane as internal standard. IR spectra were recorded using a Bruker FT-IR spectrometer IFS-113v. Samples were tested as 1 wt % mixture of the investigated salt in KBr as pressed powder pellets. UV−vis spectra were recorded on a Shimadzu UV-3101PC scanning spectrophotometer.

Diffraction patterns were obtained with a X-ray powder diffractometer Philips PW-1820, with a copper target at wavelength of 1.54 Å. Two structure simulation methods were consistently employed to determine and refine the crystal structures. The first one consists of calculation of elemental unit cells from powder pattern, assuming low symmetry of crystals, followed by verification of the Wolf's criterion.[10] The second one utilizes the least-squares method for indexing and refinement of unit cell matrix from powder data. The modified and PC adopted Pirum program was used for crystallographic calculation.[11] The single-crystal structure analysis was performed on PW 1100/20 Philips four-circle diffractometer. MoKα (λ = 0.71069 Å) radiation with graphite crystal monochromator in the incident beam was used. The calculations were done on a VAX 9000 computer employing TEXSAN software.

The nonlinear optical response of the quinolinium derivatives was evaluated by second harmonic generation from crystalline powders. A laser beam from a Q-switched Nd:YAG laser (Surelite-II, Continuum, λ = 1.064 μm, pulse width 7 ns, rep. rate 10 Hz) was directed to a sample which consists of a fine crystalline powder (typical particle size ∼3−5 μm) contained in a glass cell. The beam diameter is 1 mm, and the pulse energy is 20 mJ. The SHG signal (λ = 532 nm) generated by the powder was collected and detected by a sensitive photomultiplier tube. A reference SHG signal was taken from a 1 mm quartz crystal. Both signals are fed to a high-speed boxcar integrator card (PCI-200, Becker & Huck) and used for further evaluation. The data obtained from the organic salts were compared to urea powder of similar particle size.

The all-valence INDO/S formalism,[12] in connection with the sum-over excited particle-hole-states (SOS) formalism,[13] was employed to calculate linear and nonlinear optical properties of present cation molecules. The monoexcited configuration interaction (CIS) approximation was employed to describe the excited states. In all calculations, the lowest 160 energy transitions between SCF and CIS electronic configurations were chosen to undergo CI mixing and were included in the SOS. All calculations were performed using the ZINDO program[12] implemented on an IBM ES/9000 system. Metrical parameters used for INDO/S calculations were taken from optimized structures at AM1 level using the Gaussian 94 package[14] (AM1 option). The optimized planar molecules were oriented in the *xz* plane as illustrated in Scheme 1.

Results

Structural Properties. The crystallographic structures based on XRD powder pattern calculations are summarized in Table 1. Calculation of elemental unit cell shows that all studied salts (**2**−**5**) have the same monoclinic symmetry group *P*21/*c*, except **1** (R = CH_3O), which changed to *P*1 triclinic crystallographic point group. X-ray analysis results for the single crystal of **2** (R = CH_3) salt is shown in Figure 1 and in Table 2 (Θ and *D* are calculated intermolecular angle and distance, respectively). There are two independent molecules (totally eight molecules) in a unit cell, ρ = 1.64 g cm^{-1}, $\mu(\alpha)$ = 26.61 cm^{-1}, number of unique reflections is 5839, number of reflections with $I \geq 3\sigma_I$ is 3841, R = 0.041, R_w = 0.054. It is evident that different measured and calculated methods gave almost the same structural parameters.

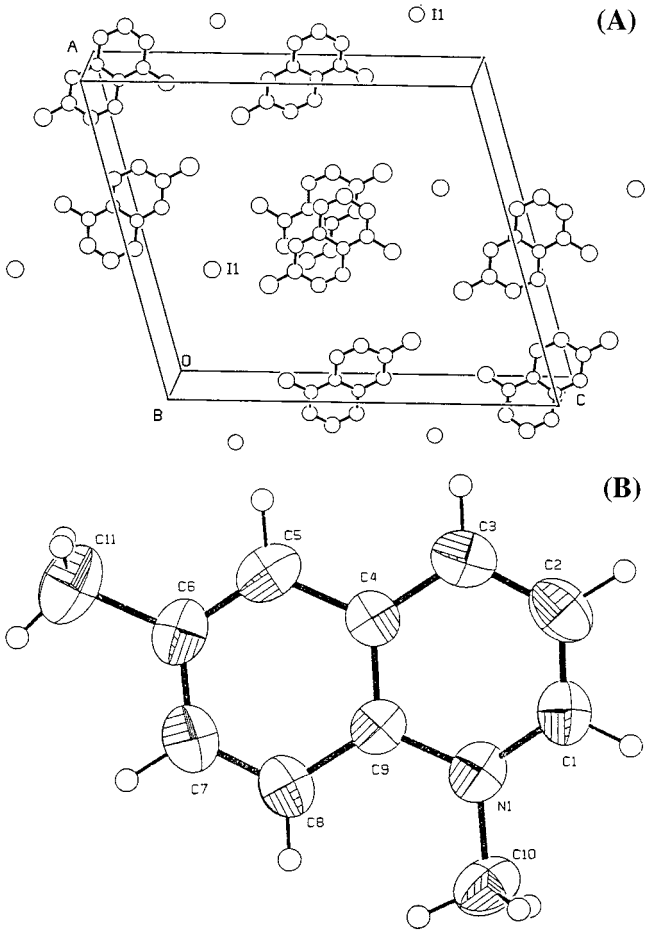

Figure 1. (A) Crystal packing and (B) structure of a single molecule of 6-methyl(*N*-methyl quinoliniumiodide) **2**.

TABLE 1: X-ray Powder Diffraction Parameters and SHG Efficiency for Quinolinium Derivatives

R	*a* (Å)	*b* (Å)	*c* (Å)	α (deg)	*β* (deg)	*γ* (deg)	*V* (Å^3)	SHG
CH_3O	31.560	8.404	10.97	93	101.00	83.56	2896.4	0.84
CH_3	17.083	7.250	19.581	90	104.63	90	2346.0	1.67
H	16.68	18.903	13.999	90	94.99	90	4303.0	3×10^{-4}
Cl	16.789	7.230	11.714	90	103.51	90	1384.5	1.67
O_2N	16.345	6.777	20.738	90	92.115	90	2295.5	9×10^{-3}

TABLE 2: Single-Crystal X-ray Data for the Methyl Quinolinium Derivative 2

R	*a* (Å)	*b* (Å)	*c* (Å)	α (deg)	*β* (deg)	*γ* (deg)	*V* (Å^3)	Θ (deg)	*D* (Å)
CH_3	17.083	7.250	19.581		104.63		2346.0	7.88	3.68

NLO Properties. The SHG intensity measured from crystalline powder samples is reported in Table 1. It indicates that SHG efficiency differs drastically with change of substituents in the quinolinium ring. Although it cannot provide the average nonlinearity coefficient unless the particle size and coherence length are known,[15] it can serve for ranking these NLO

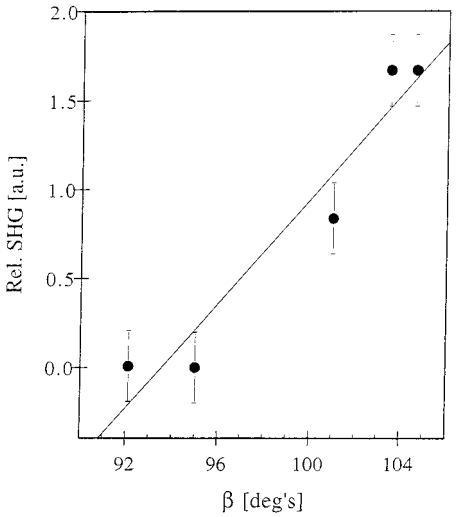

Figure 2. Relative powder SHG signal as a function of the crystallographic angle β.

TABLE 3: Spectroscopic Properties for Substituted Quinolinium Cations

R	^{1}H NMR δ (ppm) $(CH_3-N)^+$	IR ν (cm^{-1}) $(CH_3-N)^+$	UV (CT) absorption λ max (nm)	UV (CT) ϵ (M^{-1} cm^{-1})	cut off wavelength (nm)
CH_3O	4.60	1620	342	800	380
CH_3	4.57	1623	320	1200	360
H	4.66	1623	315	1300	355
Cl	4.62	1618	321	1300	355
NO_2	4.76	1633	320	900	360

materials. The largest SHG response was observed for the quinolinium derivatives with CH_3 and Cl groups, while derivatives containing H and NO_2 groups exhibit the lower SHG signal. While on the molecular level the methoxy substituent has the largest hyperpolarizability (vide infra), in the solid-state presumably dipole−dipole interaction leads to smaller β angle and hence lower NLO susceptibility. The graphic representation of SHG dependence from crystallographic angle β (Figure 2) exhibits an almost linear correlation between these parameters.

Spectral Properties. Table 3 summarizes the spectroscopic properties of the present quinolinium salts, which somehow characterize the influence of the substituent in six position on molecular polarization which, in turn, may be related to the NLO response.

The ^{1}H NMR chemical shift of the N^+-methyl protons is significantly downfield shifted for the nitro substitution due to strong deshielding effect. Analogously, IR spectra reveal the higher energy for the IR $C-N^+$ stretching frequency for **5**. It was also observed the strong influence of the nitro group on enhanced rigidity of the heterocycle.

The electronic spectra in the UV region are presented in Figure 3. The spectrum of unsubstituted quinolinium consists of two main features, an intense band centered at ~240 nm involving $\pi-\pi^*$ transitions and of a low-intensity feature centered at 320 nm, presumably involving $n-\pi^*$ excitations. Substituted compounds with weak donor (**2**) and acceptor (**4**) groups do not involve significant changes in the optical spectra, thus suggesting an analogous electronic structure. On the other hand, the stronger OMe donor (**1**) and NO_2 (**5**) acceptor substituents cause a splitting of the intense shorter wavelength band and a broadening of the low-intensity feature at longer wavelength. In particular, the band of OMe (**1**) exhibits a splitting and a bathochromic shift of 30 nm, while a tailing to the red of the same band is observed for compound (**5**). Note

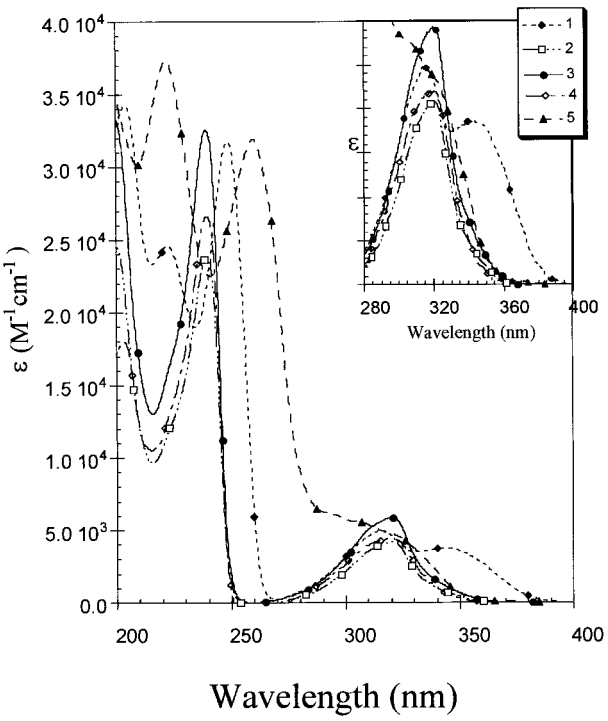

Figure 3. UV absorption spectra in H_2O of *N*-methyl quinolinium substituted iodides.

TABLE 4: Calculated Linear Optical and Nonlinear Optical Properties (in 10^{-30} cm^5 esu^{-1}) for Substituted Quinolinium Cations

R	λ_{max}, nm exptl	λ_{max}, nm calcd (f)	β_{tot} (hω = 0.0 eV)	β_{zzz} (hω = 1.17 eV)	β_{tot} (hω = 1.17 eV)
H	240	250 (0.60)	3.4	3.8	5.6
	315	317 (0.10)			
		323 (0.14)			
CH_3	320	323 (0.17)	5.0	4.4	8.1
		344 (0.08)			
OCH_3	318	324 (0.10)	6.2	6.4	11.3
	342	354 (0.10)			
Cl	321	320 (0.15)	4.4	4.3	7.0
		329 (0.09)			
NO_2	320	321 (0.15)	2.7	2.9	4.0

that the longer wavelength band of all the chromophores is located in the UV region and its absorption cut off is below 400 nm.

Theoretical Results. Frontier molecular orbitals (MOs) of cation (**3**) consist of out-of-plane π orbitals mainly delocalized over the quinolinium ring. In particular, while the HOMO, SHOMO, and SLUMO possess a predominant benzo character, the LUMO possesses a predominant pyridinium ring character. INDOS/S calculations account well for the experimental linear spectroscopic features, and a very good agreement between calculated and observed transition energies is found (Table 4). In particular, the lowest energy optical spectrum feature of the unsubstituted compound may be associated with two transitions characterized as principally $\pi-\pi^*$ (HOMO → LUMO and SHOMO → LUMO) having charge transfer character (CT) and are mainly responsible for second-order NLO response. The 6-methoxy donor substitution in the quinolinium ring results in some donor character of the frontier filled MOs. This, in turn, leads to a reduced energy gap between filled and unoccupied MOs for (**1**), which is also reflected in a calculated red-shifted lowest energy CT transition in agreement with the experimental data (Table 4). The 6-ring substitution with a weak donor or

acceptor, such as methyl or the chloro, does not result in appreciable variation of composition of frontier MOs and, hence, of optical spectra (Table 4). On the other hand, the 6-NO_2 (**5**) acceptor substitution leads to a dominant acceptor character of the SLUMO that, however, does not substantially affect the lowest energy (HOMO−LUMO) CT optical transition.

The calculated second-order hyperpolarizabilities of the present molecules are collected in Table 4. The dominant contribution to β_{tot} (the total hyperpolarizability) derives from the *zzz* component of the β_{ijk} hyperpolarizability tensor which is parallel to the CT axis (Scheme 1). The β_{tot} values of unsubstituted to NO_2-substituted compounds range from $\sim 4 \times 10^{-30}$ cm^5 esu^{-1} ($h\omega = 1.17$ eV), to $\sim 11 \times 10^{-30}$ cm^{-5} esu^{-1} ($h\omega = 1.17$ eV), similar to that of the classical donor−acceptor organic chromophore *p*-nitroaniline.[6] The calculated NLO response along the present series of materials can be related to the aforementioned CT transitions and parallels the red-shift of the lowest CT excitation, as usually observed in typical donor−acceptor organic chromophores.[6]

Discussion

We introduced the new family of quinolinium-derived acentric crystals for second-order NLO applications. The special feature of optical spectra (Figure 3) of these quinolinium derivatives is their transparency in the blue. This property is of practical importance for NLO usage including diode laser applications with $\lambda \approx 800$ nm.

Theoretical calculations revealed a reasonable fit of linear optical parameters with experimental results and predicted the appreciable SHG response of these molecules. Despite the fact that structural parameters of investigated materials do not differ a lot, the bulk SHG response changes in a range $1-10^{-4}$. On this common ground, we correlated the SHG signal with the crystallographic angle β of the elementary unit cell. The dependence of the crystal powder SHG intensity on β angle revealed an almost monotonic linear growth of SHG signal as increasing β angle. All other structural parameters have no first-order systematic effects on second order NLO properties. A possible explanation for this effect may be the dependence of crystallographic angle β with the intramolecular charge transfer axis for quinolinium derivatives. Currently we try to get all studied quinolinium derivatives in the form of single crystals to check this assumption. Supposing the existence of this dependence, the combination of present INDO/S−SOS calculations with the approach developed by J. Zyss et al.[16] can be used to predict nonlinear susceptibility.

In conclusion, we introduced a novel class of organic materials, transparent in the blue, for NLO applications. We also showed that, in addition to the nature of charge-transfer processes and intermolecular forces,[17,18] crystallographic packing is a key factor governing SHG optimization in solid-state organic compounds.

Acknowledgment. S.Y. acknowledges support for this research by the Israel Science Foundation (ISF) under Grant 651/95-2, U.S.−Israel binational science foundation (BSF) under Grant 95-0085, and the Israel Academy of Science and Humanitarians. V.B. thanks the Berg Foundation for a Post-doctoral Fellowship. S.D.B. thanks the MURST and CNR for the financial support.

References and Notes

(1) Prasad, P. N. *Contemporary Nonlinear Optics*; Academic Press: San Diego, 1992; p 265.
(2) Singer, K. D.; Sohn, J. E.; Lalama, S. L. *Appl. Phys. Lett.* **1986**, *49*, 248.
(3) Zyss, J. *Molecular nonlinear optics. Materials, physics and devices*; Academic Press, Inc.: San Diego, CA, 1994; p 201.
(4) Garito, A.; Fang, R.; Wu, M. *Phys. Today* **1994**, *6*, 51.
(5) Yoshimura T. *FUJITSU Sci. Tech.* **1991**, *27*, 115.
(6) Cheng, L.; Tam, W.; Stevenson, S.; Meredith, G.; Riken, G.; Marder S. *J. Phys. Chem.* **1995**, *95*, 10631.
(7) Nerenz, H.; Meir, M.; Grahn, W.; Reisner, A.; Schmalzin, E.; Stadler, S.; Meerholz, K.; Brauchle, C.; Jones, P. G. *J. Chem. Soc., Perkin Trans.* **1998**, *2*, 437.
(8) Zenou, N.; Zelichenok, A.; Yitzchaik, S.; Cohen, R.; Cahen, D. *Organic Thin Films*; ACS Symposium Series 695; American Chemical Society: Washington, DC, 1998; p 57.
(9) Clarke, H.; Davis, A. *Org. Synth. Colloids* **1932**, *I*, 478.
(10) Wisser, W. *J. Appl. Crystallogr.* **1969**, *2*, 89.
(11) Werne, P. *Arkiv Kemi* **1969**, *31*, 513.
(12) (a) Zerner, M.; Loew, G.; Kirchner, R.; Mueller-Westerhoff, U. *J. Am. Chem. Soc.* **1980**, *102*, 589. (b) Anderson, W. P.; Edwards, D.; Zerner, M. C. *Inorg. Chem.* **1986**, *25*, 272. (c) Bacon, A. D.; Zerner, M. C. *Theor. Chem. Acta (Berlin)* **1979**, *53*, 21. (d) Ridley, J.; Zerner, M. C. *Theor. Chim. Acta (Berlin)* **1973**, *32*, 111.
(13) (a) Di Bella, S.; Fragalü, I.; Marks, T. J.; Ratner, M. A. *J. Am. Chem. Soc.* **1996**, *118*, 12747. (b) Kanis, D. R.; Ratner, M. A.; Marks T. J. *J. Chem. Rev.* **1994**, *94*, 195.
(14) Frisch, M. J., et al. *Gaussian 94*, revision C.3; Gaussian, Inc.: Pittsburgh, PA, 1995.
(15) Kurtz, K.; Perry, T. T. *J. Appl. Phys.* **1968**, *39*, 3798.
(16) Zyss, J.; Nicould, J.; Coquillay, M. *J. Chem. Phys.* **1984**, *81*, 4160.
(17) (a) Oudar, J. L.; Zyss, J. *Phys. Rev. A* **1982**, *26*, 2016. (b) Oudar, J. L.; Zyss, J. *Phys. Rev. A* **1982**, *26*, 2028.
(18) Garito, A. F.; Lalama, S. *J. Phys. Rev. A* **1979**, *20*, 1179.